

An inhibited conformation for the protein kinase domain of the *Saccharomyces cerevisiae* AMPK homolog Snf1

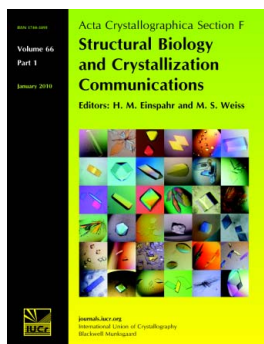
Michael J. Rudolph, Gabriele A. Amodeo and Liang Tong

Acta Cryst. (2010). **F66**, 999–1002

Copyright © International Union of Crystallography

Author(s) of this paper may load this reprint on their own web site or institutional repository provided that this cover page is retained. Republication of this article or its storage in electronic databases other than as specified above is not permitted without prior permission in writing from the IUCr.

For further information see <http://journals.iucr.org/services/authorrights.html>



Acta Crystallographica Section F: Structural Biology and Crystallization Communications is a rapid all-electronic journal, which provides a home for short communications on the crystallization and structure of biological macromolecules. It includes four categories of publication: protein structure communications; nucleic acid structure communications; structural genomics communications; and crystallization communications. Structures determined through structural genomics initiatives or from iterative studies such as those used in the pharmaceutical industry are particularly welcomed. *Section F* is essential for all those interested in structural biology including molecular biologists, biochemists, crystallization specialists, structural biologists, biophysicists, pharmacologists and other life scientists.

Crystallography Journals **Online** is available from journals.iucr.org

Michael J. Rudolph, Gabriele A.
Amodeo and Liang Tong*Department of Biological Sciences, Columbia
University, New York, NY 10027, USA

Correspondence e-mail: ltong@columbia.edu

Received 23 May 2010

Accepted 14 July 2010

PDB Reference: protein kinase domain of Snf1,
3mn3.

An inhibited conformation for the protein kinase domain of the *Saccharomyces cerevisiae* AMPK homolog Snf1

AMP-activated protein kinase (AMPK) is a master metabolic regulator for controlling cellular energy homeostasis. Its homolog in yeast, SNF1, is activated in response to glucose depletion and other stresses. The catalytic (α) subunit of AMPK/SNF1 in yeast (Snf1) contains a protein Ser/Thr kinase domain (KD), an auto-inhibitory domain (AID) and a region that mediates interactions with the two regulatory (β and γ) subunits. Here, the crystal structure of residues 41–440 of Snf1, which include the KD and AID, is reported at 2.4 Å resolution. The AID is completely disordered in the crystal. A new inhibited conformation of the KD is observed in a DFG-out conformation and with the glycine-rich loop adopting a structure that blocks ATP binding to the active site.

1. Introduction

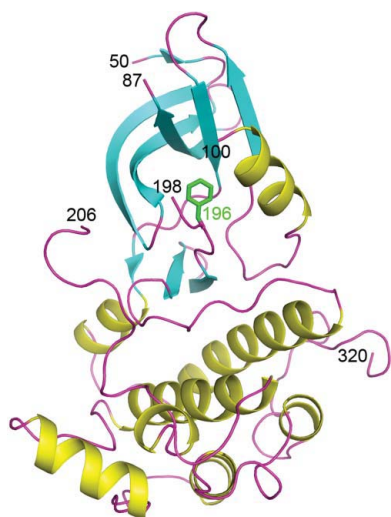
AMP-activated protein kinase (AMPK) is a key player in cellular responses to low energy levels, especially the AMP:ATP ratio (Hardie *et al.*, 1998; Kahn *et al.*, 2005; Kemp *et al.*, 2003; Hardie, 2007). The homolog of AMPK in *Saccharomyces cerevisiae*, named sucrose non-fermenting 1 (SNF1; Hardie *et al.*, 1998), has similar functions to the higher eukaryotic AMPKs, particularly under stress conditions (such as glucose depletion; Sanz, 2003). These enzymes are conserved heterotrimeric ($\alpha\beta\gamma$) in most eukaryotes (Hardie *et al.*, 1998; Kahn *et al.*, 2005; Kemp *et al.*, 2003; Hardie, 2007). The α subunit is catalytic, while the β and γ subunits are regulatory. The α subunit contains an N-terminal protein Ser/Thr kinase domain (KD; Rudolph *et al.*, 2005; Nayak *et al.*, 2006), an auto-inhibitory domain (AID; Crute *et al.*, 1998; Pang *et al.*, 2007; Chen *et al.*, 2009) and a region for interaction with the other two subunits (Fig. 1*a*). The α subunit of SNF1, known as Snf1, has a similar domain organization, with a segment (residues 330–395) that is weakly homologous to the AID in AMPK (Fig. 1*b*). Snf1 also contains a regulatory sequence (RS) just after the AID in the primary sequence (Fig. 1*a*; Jiang & Carlson, 1996).

The crystal structure of the KD–AID region of the α subunit of *S. pombe* AMPK shows that the AID forms a structure similar to that of ubiquitin-associated (UBA) domains (Chen *et al.*, 2009). The AID interacts with the linker segment between the two lobes of the KD on the opposite face from the active site of the enzyme and possibly reduces the activity of the KD by stabilizing its open conformation. The equivalent region in *S. cerevisiae* Snf1 (Fig. 1*a*) was also found to be auto-inhibitory (Chen *et al.*, 2009), although it is not known whether this AID shares a similar molecular mechanism for inhibiting SNF1. We have determined the crystal structure at 2.4 Å resolution for residues 41–440 of *S. cerevisiae* Snf1 (containing the KD and the AID). The AID was completely disordered in this crystal, although we did observe a new inhibited conformation for the KD.

2. Materials and methods

2.1. Protein expression and purification

Residues 41–440 of *S. cerevisiae* Snf1 were subcloned into the pET28a vector and overexpressed in *Escherichia coli* BL21-Gold (DE3) at 293 K. The soluble protein was purified by nickel-affinity



chromatography and then treated with 2 mM dimethylamine–borane (DMAB) and 1.5% (v/v) formaldehyde to methylate the lysine side chains (Rayment, 1997). The protein was further purified by gel-filtration chromatography, concentrated to 25 mg ml⁻¹ in a solution containing 20 mM Tris pH 7.5, 200 mM NaCl, 5 mM DTT and 5% (v/v) glycerol and stored at 193 K.

2.2. Crystallization, data collection and structure determination

Crystals of Snf1 (41–440) were obtained at 294 K by the sitting-drop vapor-diffusion method. The initial crystallization condition was identified by sparse-matrix screening using a collection of commercially available kits. The protein was at 25 mg ml⁻¹ concentration. The reservoir solution contained 10% (w/v) PEG 3350 and 50 mM Na₂SO₄. The drop was formed by mixing 1 µl protein solution with 1 µl reservoir solution. This condition is somewhat similar to that reported previously for the crystallization of the KD only [100 mM Tris pH 8.5, 25% (w/v) PEG 3350 and 300 mM ammonium sulfate; Rudolph *et al.*, 2005], although the crystals are not isomorphous. The crystals were cryoprotected by the introduction of 30% (v/v) ethylene glycol and flash-frozen in liquid nitrogen for data collection at 100 K. The crystals belonged to space group *I*4₁22, with unit-cell parameters *a* = *b* = 77.0, *c* = 286.2 Å. There is one molecule of Snf1 in the asymmetric unit.

Table 1

Summary of crystallographic information.

Values in parentheses are for the highest resolution shell.

Resolution range (Å)	30–2.4 (2.5–2.4)
No. of observations	105478
<i>R</i> _{merge} (%)	12.3 (34.9)
<i>I</i> / <i>σ</i> (<i>I</i>)	11.9 (3.1)
Redundancy	6.1 (5.9)
No. of reflections	16477
Completeness (%)	99 (97)
<i>R</i> factor (%)	23.0 (30.0)
Free <i>R</i> factor† (%)	24.6 (34.6)
Ramachandran plot statistics	
Residues in most favored region (%)	91.3
Residues in additional allowed region (%)	8.2
Residues in disallowed region	None
No. of atoms	
Protein	2040
Solvent waters	54
Average temperature-factor value (Å ²)	
Protein	60
Solvent	56
R.m.s.d. in bond lengths (Å)	0.010
R.m.s.d. in bond angles (°)	1.3

† 5% of reflections were selected randomly for free *R* calculation.

X-ray diffraction data were collected to 2.4 Å resolution on the X4C beamline of the National Synchrotron Light Source (NSLS). The diffraction images were processed with the *HKL* package

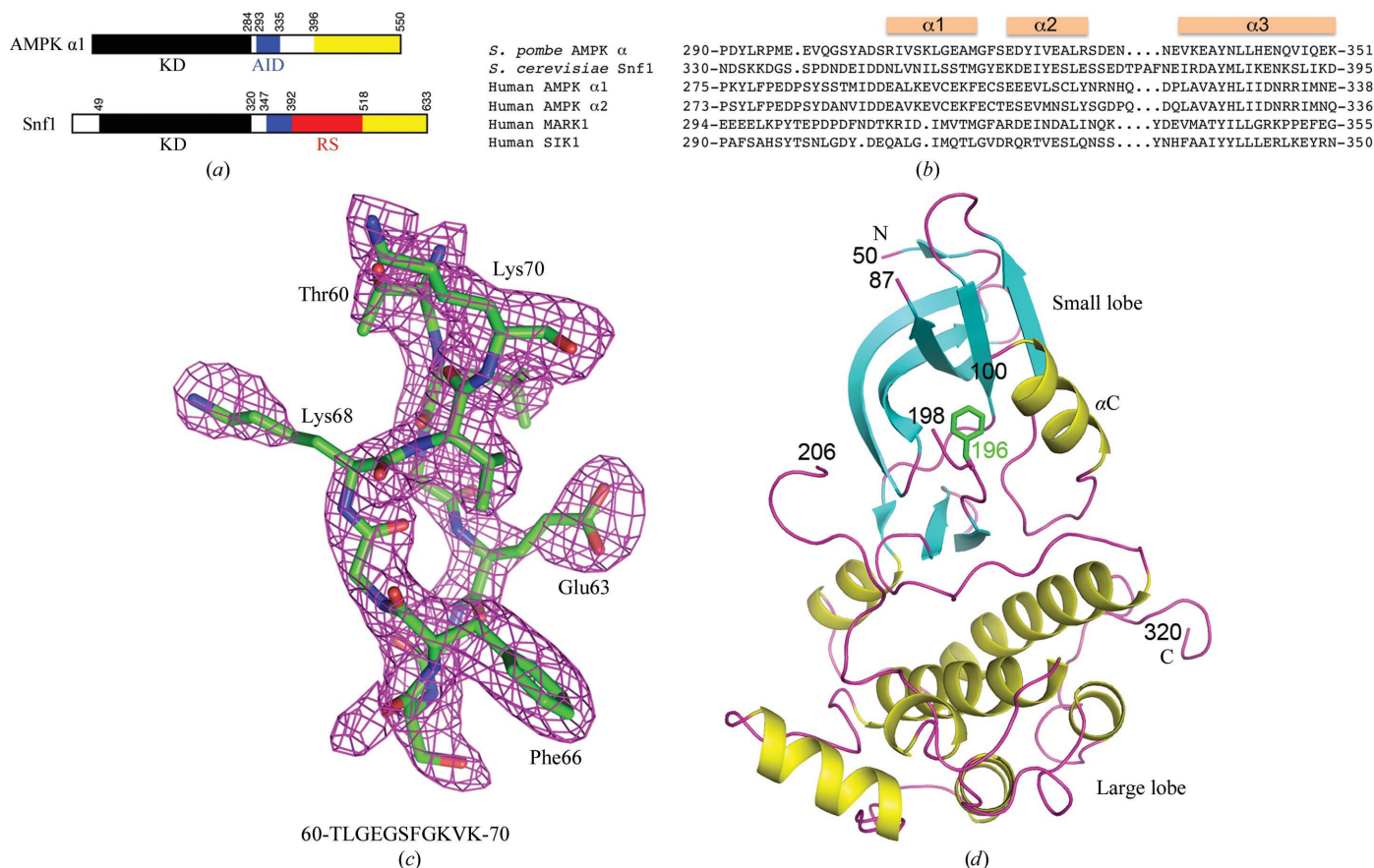


Figure 1

A new structure of the *S. cerevisiae* Snf1 KD. (a) Domain organizations of the $\alpha 1$ subunit of mammalian AMPK and *S. cerevisiae* Snf1. The protein kinase domain (KD) is in black, the auto-inhibitory domain (AID) is in blue, the regulatory sequence (RS) is in red and the region for interaction with the β subunits is in yellow. (b) Sequence alignment of the AIDs of *S. pombe* AMPK, *S. cerevisiae* Snf1, human AMPK $\alpha 1$ and $\alpha 2$ subunits, human MARK1 and human SIK1. The three helices observed in the *S. pombe* AMPK structure are indicated. (c) Overall structure of the *S. cerevisiae* Snf1 KD (residues 50–320). The side chain of Phe196 in the DFG motif is shown in green. The crystal contained residues 41–440 of Snf1, but the C-terminal segment, including the AID, is disordered. (d) OMIT $F_o - F_c$ electron density for the glycine-rich loop at 2.4 Å resolution, contoured at 3σ . The structural figures were produced with *PyMOL* (<http://www.pymol.org>).

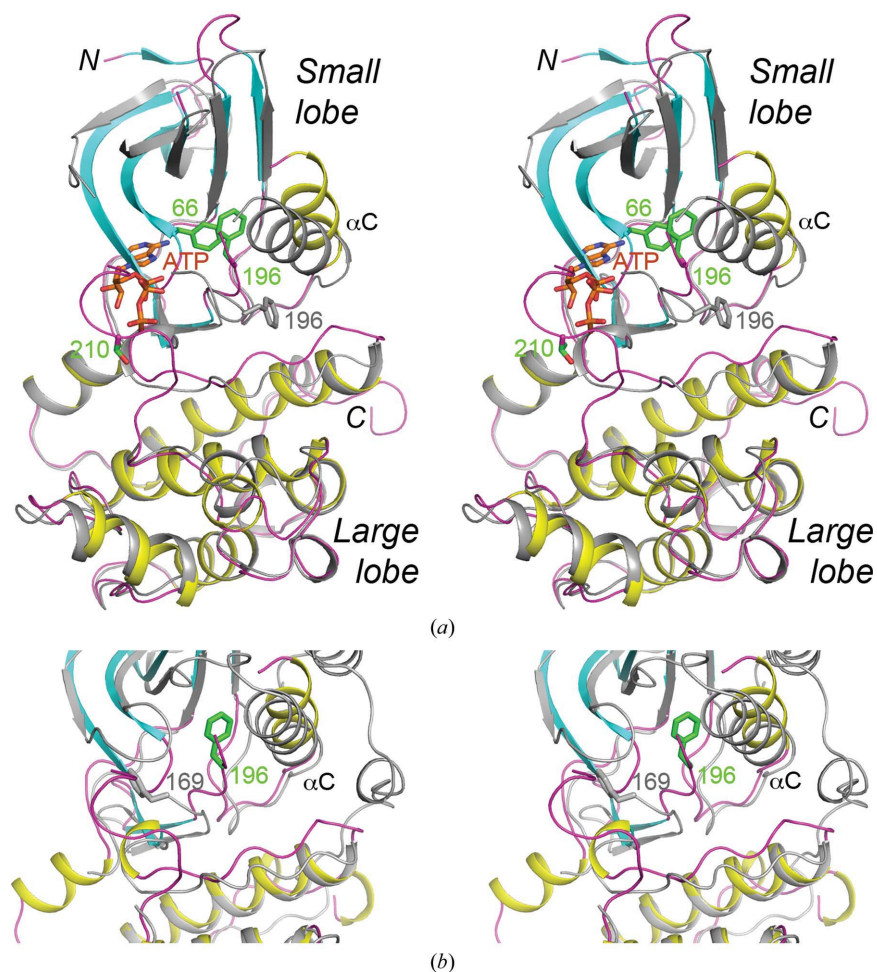


Figure 2

Comparisons to other structures. (a) Overlay of the new KD structure (in color) with the KD structure reported previously (in gray; Rudolph *et al.*, 2005). The side chains of Phe66 (glycine-rich loop), Phe196 (DFG motif) and Thr210 (phosphorylation site) in the new structure are shown in green and the side chain of Phe196 in the previous structure is shown in gray. The new KD structure assumes a DFG-out conformation. The expected bound position of ATP is also shown. (b) Overlay of the new KD structure (in color) with that of p38 MAP kinase in a DFG-out conformation (in gray; Pargellis *et al.*, 2002). Only the active-site region is shown. The side chains of Phe196 in Snf1 KD (in green) and the equivalent Phe169 in p38 (in gray) have clear differences in their positions.

(Otwinowski & Minor, 1997). The structure was solved by the molecular-replacement method with the program *COMO* (Jogl *et al.*, 2001), using the structure of the *S. cerevisiae* KD as the model (Rudolph *et al.*, 2005). The model was modified to fit the electron density and additional residues that were not in the search model were located. Structure refinement was carried out with the programs *CNS* (Brünger *et al.*, 1998) and *REFMAC* (Murshudov *et al.*, 1997). Manual rebuilding of the atomic model was performed with the program *O* (Jones *et al.*, 1991). The crystallographic information is summarized in Table 1.

3. Results and discussion

3.1. Crystal structure of residues 41–440 of Snf1

The crystal structure of residues 41–440 of *S. cerevisiae* Snf1, covering the KD–AID region (Fig. 1a), has been determined at 2.4 Å resolution. Reductive methylation of the lysine residues in the protein (Rayment, 1997) was used to obtain crystals that diffracted to high resolution, as crystals grown from protein without methylation only diffracted to about 3.6 Å resolution (Rudolph *et al.*, 2005). The atomic model has good agreement with the observed diffraction data as well as expected bond lengths, bond angles and other geometric

parameters (Table 1). No clear electron density was observed for any of the methyl groups in the lysine side chains, although some of them did show bulkier electron density for the NZ atom, suggesting that the methyl groups are likely to be disordered.

The current atomic model contains residues 50–87, 100–198 and 206–320 of the KD (Fig. 1c). Residues 321–440 in the C-terminal segment, including the AID, are disordered in this crystal as no electron density was observed for them. It is unlikely that the AID was removed by proteolysis during crystallization, as we did not observe any evidence of proteolysis during the overnight incubation for reductive methylation and the crystal used for data collection grew to full size within 48 h.

The disordering of the AID in these new crystals is consistent with our previous observations on crystals of the unmethylated protein in a different crystal form in which the AID is also disordered (Rudolph *et al.*, 2005). These observations contrast with those on the *S. pombe* AID (Chen *et al.*, 2009). The KD–AID conformation observed for *S. pombe* AMPK may not be compatible with the current crystal, as the last five residues of the AID in that conformation clash with another molecule of *S. cerevisiae* KD in the current crystal. This may also suggest that the interactions between the KD and AID are weaker in *S. cerevisiae* Snf1 compared with the *S. pombe* enzyme, as they cannot compete against crystal packing. Snf1 also has a longer

loop between helices $\alpha 2$ and $\alpha 3$ in the AID (Fig. 1*b*), which may also have an impact on its conformation and explain the disordering of the AID in Snf1.

3.2. A new conformation for the KD of Snf1

The new structure of the Snf1 KD shows several significant differences from the KD structure that we reported previously (Fig. 2*a*; Rudolph *et al.*, 2005) obtained from a crystal containing residues 41–315. In the small lobe of the KD, the glycine-rich loop (residues 62–68, which interacts with the phosphates of ATP) is well ordered in the new structure, with well defined electron density (Fig. 1*d*), while it was disordered in the previous structure (Fig. 2*a*). The average temperature-factor value for the residues in this loop is around 60 Å², while that for residues in the core of the structure is about 50 Å². The loop in this conformation is far from the crystal-packing interface and is therefore unlikely to be stabilized by it. Most importantly, the residues at the tip of this loop are positioned into the groove between the two lobes, which would be expected to block ATP binding (Fig. 2*a*) and could represent another mechanism of auto-inhibition for the KD. There is also a large difference in the positioning of the αC helix and the small lobe is slightly more open in the new structure as it is rotated further away from the large lobe (Fig. 2*a*).

In the large lobe, the conserved DFG motif just prior to the activation segment (residues 188–218) assumes a DFG-out conformation in the new structure (Pargellis *et al.*, 2002), while it assumes the DFG-in conformation in the previous structure. This DFG-out conformation is distinct from that reported previously (Fig. 2*b*) and the Phe196 residue in this motif does not clash with the ATP molecule (Fig. 2*a*). The new conformation of the glycine-rich loop is incompatible with the DFG-out conformation observed previously (Fig. 2*b*). The rearrangement of the DFG segment is probably linked to the change in the positioning of the αC helix (residues 97–109) in the small lobe and the Phe196 residue is also placed near Phe66 in the glycine-rich loop (Fig. 2*a*).

A large part of the activation segment of the KD, including Thr210 that is phosphorylated for activation, is ordered in the new structure. These residues are positioned far from the rest of the KD (Fig. 1*c*). Instead, they are located in the interface of a crystallographic dimer, which is similar to the KD dimer observed previously (Rudolph *et al.*, 2005; Nayak *et al.*, 2006). Finally, two loops in this lobe, residues 220–229 just after the activation segment and residues 172–180, also show large conformational differences between the two structures (Fig. 2*a*).

Most of the differences described above are also observed when this new structure is compared with another previously reported structure of the Snf1 KD (Nayak *et al.*, 2006). In this previous

structure the KD assumes the DFG-in conformation, although the αC helix is positioned even further away; it is in a position close to that of the αC helix in the *S. pombe* KD–AID structure (Chen *et al.*, 2009). A large part of the activation segment is also observed but in a different conformation.

Overall, the DFG-out conformation and the positioning of the glycine-rich loop and the αC helix indicate that this new structure of the Snf1 KD is in an inactive inhibited conformation. Further studies are needed to reveal the molecular mechanism by which the AID and the rest of the heterotrimer contribute to the regulation of SNF1.

We thank Randy Abramowitz and John Schwanof for setting up the X4C beamline. This research was supported in part by NIH grant DK067238 (to LT). GAA was also supported by an NIH training program in molecular biophysics (GM008281).

References

- Brünger, A. T., Adams, P. D., Clore, G. M., DeLano, W. L., Gros, P., Grosse-Kunstleve, R. W., Jiang, J.-S., Kuszewski, J., Nilges, M., Pannu, N. S., Read, R. J., Rice, L. M., Simonson, T. & Warren, G. L. (1998). *Acta Cryst.* **D54**, 905–921.
- Chen, L., Jiao, Z.-H., Zheng, L.-S., Zhang, Y.-Y., Xie, S.-T., Wang, Z.-X. & Wu, J.-W. (2009). *Nature (London)*, **459**, 1146–1149.
- Crute, B. E., Seefeld, K., Gamble, J., Kemp, B. E. & Witters, L. A. (1998). *J. Biol. Chem.* **273**, 35347–35354.
- Hardie, D. G. (2007). *Nature Rev. Mol. Cell Biol.* **8**, 774–785.
- Hardie, D. G., Carling, D. & Carlson, M. (1998). *Annu. Rev. Biochem.* **67**, 821–855.
- Jiang, R. & Carlson, M. (1996). *Genes Dev.* **10**, 3105–3115.
- Jogl, G., Tao, X., Xu, Y. & Tong, L. (2001). *Acta Cryst.* **D57**, 1127–1134.
- Jones, T. A., Zou, J.-Y., Cowan, S. W. & Kjeldgaard, M. (1991). *Acta Cryst.* **A47**, 110–119.
- Kahn, B. B., Alquier, T., Carling, D. & Hardie, D. G. (2005). *Cell Metab.* **1**, 15–25.
- Kemp, B. E., Stapleton, D., Campbell, D. J., Chen, Z.-P., Murthy, S., Walter, M., Gupta, A., Adams, J. J., Katsis, F., van Denderen, B., Jennings, I. G., Iseli, T., Mitchell, B. J. & Witters, L. A. (2003). *Biochem. Soc. Trans.* **31**, 162–168.
- Murshudov, G. N., Vagin, A. A. & Dodson, E. J. (1997). *Acta Cryst.* **D53**, 240–255.
- Nayak, V., Zhao, K., Wyce, A., Schwartz, M. F., Lo, W. S., Berger, S. L. & Marmorstein, R. (2006). *Structure*, **14**, 477–485.
- Otwinowski, Z. & Minor, W. (1997). *Methods Enzymol.* **276**, 307–326.
- Pang, T., Xiong, B., Li, J.-Y., Qiu, B.-Y., Jin, G.-Z., Shen, J.-K. & Li, J. (2007). *J. Biol. Chem.* **282**, 495–506.
- Pargellis, C., Tong, L., Churchill, L., Cirillo, P. F., Gilmore, T., Graham, A. G., Grob, P. M., Hickey, E. R., Moss, N., Pav, S. & Regan, J. (2002). *Nature Struct. Biol.* **9**, 268–272.
- Rayment, I. (1997). *Methods Enzymol.* **276**, 171–179.
- Rudolph, M. J., Amodeo, G. A., Bai, Y. & Tong, L. (2005). *Biochem. Biophys. Res. Commun.* **337**, 1224–1228.
- Sanz, P. (2003). *Biochem. Soc. Trans.* **31**, 178–181.